Sains Malaysiana 50(6)(2021): 1685-1695
http://doi.org/10.17576/jsm-2021-5006-15

Preliminary Study on Effect of Hydrothermal Temperature during TiO_2 Synthesis on the Biodiesel Production from Waste Cooking Oil

(Kajian Awal Kesan Suhu Hidroterma semasa Sintesis TiO_2 terhadap Penghasilan Biodiesel daripada Sisa Minyak Masak)

NURASHINA ABDUL RAHMAN, ANITA RAMLI* & CHONG FAI KAIT

ABSTRACT

In the present work, effect of hydrothermal temperature from 120 to 160 °C on TiO_2 physicochemical properties as well as its photocatalytic activity towards biodiesel production using waste cooking oil (WCO) was investigated. TiO_2 was synthesized via hydrothermal method using Titanium butoxide, $Ti(OBu)_4$ as the precursor and nitric acid, HNO_3 as the peptizing agent. Next, the synthesized photocatalyst was dried at 60 °C for 24 h and later calcined at 400 °C for 2 h. The synthesized TiO_2 was characterized using X-ray diffraction (XRD) and Burnauer- Emmet- Teller (BET) to determine their crystallinity and textural properties. Results showed that all synthesized TiO_2 have a mixture of anatase and rutile phase and N_2 adsorption- desorption isotherm for all catalyst possess Type IV isotherm according to IUPAC classification with hysteresis loop of type H1. Then, all the synthesized catalysts were tested for biodiesel production using esterified waste cooking oil under visible light irradiation for 1 h and 10 min. Percentage of fatty acid methyl ester (FAMEs) present in the synthesized biodiesel was determined using gas chromatography with flame ionization detector (GC-FID). The synthesized catalyst (T24_160) showed a good photocatalytic activity as the percentage of biodiesel yield was higher (3.41%) compared to the other catalyst.

Keywords: Biodiesel; hydrothermal temperature; photocatalyst; physicochemical properties; TiO_2

ABSTRAK

Kesan suhu hidroterma daripada 120 sehingga 160 °C ke atas sifat fizikokimia TiO_2 serta aktiviti pemfotomangkinan terhadap penghasilan biodiesel dengan menggunakan minyak terpakai (WCO) telah dikaji. TiO_2 telah disintesis melalui kaedah hidroterma dengan menggunakan Titanium butoksida, $Ti(OBu)_4$ sebagai prekursor dan asid nitrik, HNO_3 sebagai agen peptitasi. Fotomangkin yang disintesis telah dikeringkan pada suhu 60 °C selama 24 jam dan kemudian telah terkalsin pada suhu 400 °C selama 2 jam. TiO_2 yang telah disintesis dicirikan menggunakan pembelauan sinar- X (XRD) dan Burnauer- Emmet- Teller (BET) untuk menentukan kehabluran dan sifat tekstur fotomangkin tersebut. Hasil kajian mendapati bahawa kesemua mangkin TiO_2 disintesis menunjukkan campuran fasa anatas dan rutil serta isoterma penjerapan-penyahjerapan N_2 menujukkan isoterma jenis IV berdasarkan pengelasan IUPAC dengan gelung histeresis jenis H1. Seterusnya, kesemua mangkin disintesis telah diuji untuk penghasilan biodiesel menggunakan minyak terpakai yang telah diesterifikasi di bawah sinaran cahaya nampak selama 1 jam 10 min. Peratus asid lemak metil ester (FAMEs) hadir di dalam biodiesel disintesis telah ditentukan dengan menggunakan gas kromatografi - pengesan pengionan nyala (GC- FID). Mangkin yang disintesis (T24_160) menunjukkan aktiviti pemfotomangkinan yang baik dengan peratusan hasil biodiesel lebih tinggi (3.41 %) berbanding dengan mangkin yang lain.

Kata kunci: Biodiesel; fotomangkin; sifat fizikokimia; suhu hidroterma; TiO_2

INTRODUCTION

Past few years, crisis on non-renewable energy becoming serious as the demand for the energy consumption for global industrialization increasing day by day (Habibullah et al. 2015). As it is known, most of the power consumption in the world comes from fossil fuels sources like petroleum, coal and natural gas. However, these non-renewable sources will be exhausted in the future. By knowing that energy

play a major role for globalization, research on introducing new energy which is renewable and sustainable alternative energy sources has become more intense as it is not only solving on shortage of non-renewable energy but able to overcome environmental concerns such as pollution and global warming caused by burning of fossil fuel (Demirbas 2005). Among the renewable energy resources such as solar, wind, biomass and geothermal, biodiesel which is derived from biomass has garner attention due to its environmental benefits such as low CO_2 emission that will help in overcoming global warming (Firoz 2017), zero toxicity, highly degradable and does not release hydrocarbons (Mishra & Goswami 2018). The fuel is also essentially free from sulfur and aromatics, producing lower exhaust emissions and highly oxygenated compared to the petroleum diesel even though it has almost the same properties in terms of fuel efficiency (Demirbas 2009).

Biodiesel is known as mono-alkyl ester of long fatty acid that derived from vegetable oils or animal fats (Gashaw et al. 2015). Common feedstocks that have been used in the production of biodiesel are soybean oil, palm oil, animal fats, coconut oil, rapeseed, sunflower, and olive oil (Balat & Balat 2010). However, due to several problems related to the use of edible oil as biodiesel feedstock, researchers have come out with another way to replace the edible oil with non-edible oils, micro-algae and waste cooking oil. Among them, waste cooking oil is seen more economical compared to the other feedstocks.

Transesterification is a common method used these days to produce biodiesel, involving a chemical reaction between triglycerides present in vegetable oil, animal fat or waste cooking oil with alcohol (i.e. methanol) in the presence of catalyst such as homogenous and heterogeneous catalysts. Conventional homogenous catalyst is widely used in industrial field to produce biodiesel (Lau et al. 2016). However, several problems arise as the homogeneous catalysts are difficult to separate from the biodiesel mixture, causing corrosion to the reactor and formation of soap (Firoz 2017). In order to overcome these problems, an alternative method is needed by introducing heterogeneous catalyzed transesterification to facilitate biodiesel production.

Photocatalysis using heterogeneous catalyst have been widely applied in water splitting process for hydrogen production, degrading pollutant in water, and carbon dioxide reduction (Santhosh et al. 2018; Tentu & Basu 2017; Tjandara & Huang 2018). Discovery of photo-activated water splitting using titanium dioxide, TiO_2 by Fujishima and Honda in 1972 has led to intense study on heterogeneous photocatalyst. Heterogeneous photocatalysis is known as a catalytic process that initiated by the presence of light (Ibhadon & Fitzpatrick 2013). Recently, Corro et al. (2017) have investigated the use of Cr/SiO_2 as photocatalyst in biodiesel production by solar irradiation. Generally, catalyst has been added in a chemical process to speeds up the reaction. However, in photocatalysis system, the catalyst was used to convert the solar energy to chemical energy by oxidizing or reducing the material to a useful substance (Nakata & Fujishima 2012).

Among the semiconductor photocatalyst, TiO_2 has garner attention for its high resistance to photo-corrosion, chemically stable and has high photocatalytic activity. TiO_2 is known for having three types of crystalline phase namely anatase, rutile, and brookite. Study on TiO_2 shows that, anatase phase has higher photocatalytic activity as compared to rutile and brookite phases (Fischer et al. 2017; Liao & Que 2010; Zhang et al. 2014). On the other hand, rutile phase is chemically stable as compared to the anatase and brookite which are metastable (Hu et al. 2003). In order to get a catalyst that has high photocatalytic activity, the synthesis method with proper reaction conditions is required. Sol-gel method has been widely used to synthesis TiO_2 as the method is simple and more economical (Sharma et al. 2014). In another study, hydrothermal method was reported to produce a well-crystalline photocatalyst under moderate condition (Lencka & Riman 1995).

This current study gives insight on the effect of hydrothermal temperature in synthesizing TiO_2 on their corresponding activity in solar-irradiation driven biodiesel production using waste cooking oil as the feedstock.

Materials and Methods

Materials and Chemicals

Titanium (IV) butoxide ($Ti(OBu)_4$, 97%), 2- propanol (99.5%), Nitric acid (HNO_3, 65%), Sulfuric acid (H_2SO_4, 95- 97%), Methanol (≥ 99.5%), Potassium hydroxide pellets (≥ 85%), Diethyl ether (≥ 98%), Ethanol (95%) were purchased from Sigma Aldrich and used without further purification.

Hydrothermal Synthesis of TiO_2

TiO_2 nanoparticles was synthesized using titanium butoxide $Ti(OBu)_4$ as the precursor. 25 mL of $Ti(OBu)_4$ was added slowly into 8 mL of 2-propanol and the mixture was stirred for 5 min. Then, the mixture was added dropwise into a beaker containing 200 mL of distilled water under stirring and the stirring was continued for another 30 min. Afterward, 3 mL of concentrated HNO_3 was added into the mixture under vigorous stirring for 30 min. The mixture

was then transferred into Teflon- lined autoclave and heated at various temperature (120, 140, and 160 °C) for 24 h. The powder slurry TiO_2 mixture formed was then filtered and washed several times with 2-propanol and distilled water followed by drying at 60 °C for 24 h and calcination at 400 °C for 2 h at a heating rate of 5 °C/min. The synthesized TiO_2 was denoted as T24_120, T24_140 and T24_160.

CATALYST CHARACTERIZATION

The synthesized TiO_2 was characterized using powder X-ray diffraction (XRD) on Bruker AXS D8 Advance Diffractometer with Mn filtered Cu- Kα at angle range between 15-80° to determine its crystallite structure. The crystallite size of the catalysts was calculated using Scherer equation in (1) and is tabulated in Table 1.

$$D = \frac{k\lambda}{\beta \cos\theta} \quad (1)$$

where D is the crystallite size; k the Scherrer constant; λ is the wavelength of the X- ray source; β is full width half maximum (FWHM) in radian; and θ is the peak position. Besides, the polymorph composition of the photocatalyst was derived from Su et al. (2011) as in (2).

$$[A]/\% = \frac{100 \times I_A}{I_A + 1.265 \times I_R} \quad (2)$$

where I_A and I_R correspond to the area of anatase (101); and rutile (110) XRD peaks. On the other hand, the rutile content can be refer to (3).

$$[R] = 100 - [A] \quad (3)$$

The surface area, total pore volume and pore volume distribution were acquired from nitrogen adsorption-desorption isotherms using an adsorption porosimeter (Micromeritics ASAP 2020) at 78K. The samples were degassed at 200 °C for 4 h prior to the measurement. The surface area was calculated using Multi-Point Brunnauer-Emmet-Teller method (BET) when monomolecular layer is established over the entire sample surface. Pore volume was calculated at a relative pressure $P/P^o = 0.99$, assuming full surface saturation with nitrogen. The average pore diameter and the pore size distribution of catalysts were calculated from the desorption isotherms data using Barret-Joyner-Halenda (BJH) method.

CHARACTERIZATION OF FEEDSTOCK

The waste cooking oil (WCO) was collected from a restaurant in Ipoh where the waste cooking oil was used for frying purpose. Prior to use, the feedstock was filtered using fine screen cloth to separate any insoluble impurities and washed several times using hot water to remove salt and other soluble materials. Then, the feedstock was dried in oven an at 105 °C for 2 h.

The acid value of the WCO was determined using the European standard EN14104 method (Olutoye & Hameed 2011). This method consists of dissolving 1 g of oil in a mixture of diethyl ether and ethanol with 1:1 ratio in the presence of phenolphthalein as the indicator. Then, the mixture was titrated against 0.1 N standard aqueous solution of KOH until definite pink color persisted for 10 s. The acid value (mg KOH per g oil sample) was calculated using (4).

$$\text{Acid value (mg KOH/ g of oil)} = \frac{A \times N \times 56.1}{W} \quad (4)$$

where 56.1 is the molecular weight of KOH (g/mol); N is the normality of KOH (mEq/mL); A is the volume of the KOH (mL) used for titration; and W is the mass of the oil sample (g).

Water content is known as one of the physicochemical properties which may affect the transesterification reaction and biodiesel yield. The presence of water in the feedstock can cause side reaction such as soap formation when the reaction was carried out using base catalyst (Tan et al. 2010). Therefore, in order to avoid the formation of soap, the feedstock used should be free from water or at least having water content lower than 0.3 wt. % (Kusdiana & Saka 2004; Lotero et al. 2005). The Karl-Fischer titration method was used to determine the water content in oil sample. The analysis was performed using a coulometric Karl Fischer titrator, DL 39 (Mettler Toledo, meet ASTM D6304- 07) with Hydranal coulomat AG reagent (Riedel-de Haen). Prior to measurement of water content, the oil sample was dried in a vacuum oven for 24 h at 80 °C, then, 3 g of oil sample was injected into the instrument. The measurements were taken in triplicate and the average value was reported.

BIODIESEL PRODUCTION UNDER SOLAR IRRADIATION

The photo-esterification of free fatty acid (FFA) in waste cooking oil was performed in a photo- reactor equipped with condenser and Xenon lamp to stimulate the visible light from sunlight. The methanol to oil ratio was 4:1 following the work reported by Cassallas et al. (2018) with 1 wt. % catalyst loading with respect to the feedstock. The reaction was carried out for a total of 1 h and 10 min using concentrated sulfuric acid (H_2SO_4) as catalyst. At the end of the reaction, the mixture was transferred into a separating funnel. The bottom layer contains a mixture

of fatty acid methyl ester (FAME) produced from the photo-esterification of FFA and any unreacted feedstock. The upper layer consists of a mixture of methanol, water, glycerol and H_2SO_4. The mixture of photo-esterified FFAs and unreacted triglyceride was washed using hot water (70-80 °C) several times and dried in oven at 105 °C for 2 h. The esterified oil was transferred back into the photo-reactor for photo-transesterification using the synthesized heterogeneous catalyst, T24_120 at catalyst loading of 1.0 wt. % and 6:1 methanol to oil ratio for 1 h and 10 min. Finally, the mixture was kept overnight to separate the layer of FAME produced from the photocatalyst, unreacted methanol and glycerol. The FAME produced was collected and washed with hot water and dried in oven at 105 °C for 2 h. The same method was repeated by replacing T24_120 catalyst with T24_140 and T24_160 catalysts. Then, the biodiesel yield was measured using Shimadazu GC-2010 equipped with flame ionization detector (GC-FID) fitted with BPX- 20 column using Helium (He) as the carrier gas at the flow rate of 1.73 mL/min and pressure of 83.9 kPa. The column temperature was initially set at 150 °C and increased to 240 °C at heating rate 5 °C/min while both the injector and FID temperature were set to 250 °C. The biodiesel yield (%) was calculated using (5) and (6).

$$\text{FAME Content (\%)} = \frac{\sum A - A_S}{A_S} \times \frac{C_S V_S}{m} \times 100\% \quad (5)$$

where $\sum A$ is the sum of signal areas of fatty acid methyl ester (FAME); A_S is the signal area of methyl heptadecanoate (C17); C_S is the concentration of methyl heptadecanoate; V_S is the volume of standard solution; and m is the mass of the biodiesel

$$\text{FAME Yield (\%)} = \text{FAME content from GC} \times \frac{\text{weight of biodiesel}}{\text{weight of WCO}} \times 100 \quad (6)$$

Results and Discussion

Crystalinity of TiO_2

Figure 1 shows the XRD diffractogram for TiO_2 synthesized at different hydrothermal temperatures. Two major peaks were observed in all samples which is anatase peak at $2\theta = 25.4°$ assigned to TiO_2 (1 0 1) plane and rutile peak at $2\theta = 27.5°$ assigned to TiO_2 (1 1 0) plane. According to Scanlon et al. (2013), mixed phase of anatase and rutile in TiO_2 will show high photocatalytic activity compared to single constituents of TiO_2 due to synergistic effect, however, the reason on synergistic effect still remain elusive. As the hydrothermal temperature increased, no significant changes on the anatase peak was observed but the rutile peak becomes narrower which indicate an increased in crystallinity. High growth temperature would be able to provide enough thermal energy to the carriers to accommodate on the lattice sites (Hussain et al. 2019).

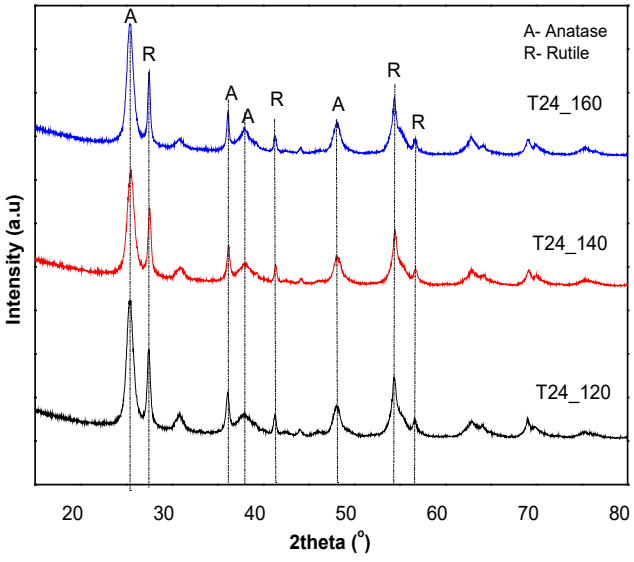

FIGURE 1. XRD pattern for mesoporous TiO_2 prepared at different hydrothermal temperature

Table 1 shows that the increment in hydrothermal temperature from 120 to 160 °C does not have significant effect on the crystallite size of anatase crystals while the crystallite size of the rutile phase increased with increasing hydrothermal temperature. Increasing crystal size of rutile when the hydrothermal temperature increase might be due to nanocrystal coalescence that take place (Collazo et al. 2011). Furthermore, the ratio between anatase and rutile observed which the percentage of anatase increasing meanwhile rutile decreasing as the hydrothermal temperature increased. According to Su et al. (2011), the optimum mixture is found to be 60% anatase and 40% rutile as the catalytic activity increased by approximately 50% as compared to pure anatase TiO_2. Furthermore, Su et al. (2011) also reported that the anatase ratio must be maintained to below 80% as the rutile phase is required for electron-hole pair separation.

TABLE 1. Crystal size calculated using Scherrer equation and anatase to rutile ratio for T24_120, T24_140 and T24_160

Catalyst	Crystallite size (nm)		Anatase to rutile ratio
	Anatase	Rutile	
T24_120	10.4	27.7	64.6: 35.4
T24_140	9.9	30.6	70.4: 29.6
T24_160	10.8	38.7	71.2: 28.8

SURFACE AREA AND POROSITY ANALYSIS

Figure 2 shows the N_2 adsorption-desorption isotherm plot for all the synthesized TiO_2 catalysts where the catalysts showed type IV isotherm according to IUPAC classification with hysteresis loop of type H1 at relative pressure (P/P^o) between 0.65 and 0.95 which indicated the formation of mesoporous TiO_2 material. This clearly shows that the catalysts are mesoporous which connected to the aggregation of TiO_2 crystallite in the nanoparticles (Malligavathy et al. 2018). The textural properties of the synthesized TiO_2 is shown in Table 2. Although no significant changes on the surface area and pore volume of the synthesized TiO_2 was observed, the increased in hydrothermal temperature from 120 to 160 °C resulted in slight increment in the average pore size. Singh and Birajdar (2017) reported that increased in surface area and pore volume would increase the transfer of surface charge carriers and decreased the recombination of electron-hole pair, which eventually would increase the photocatalytic activity of the catalyst.

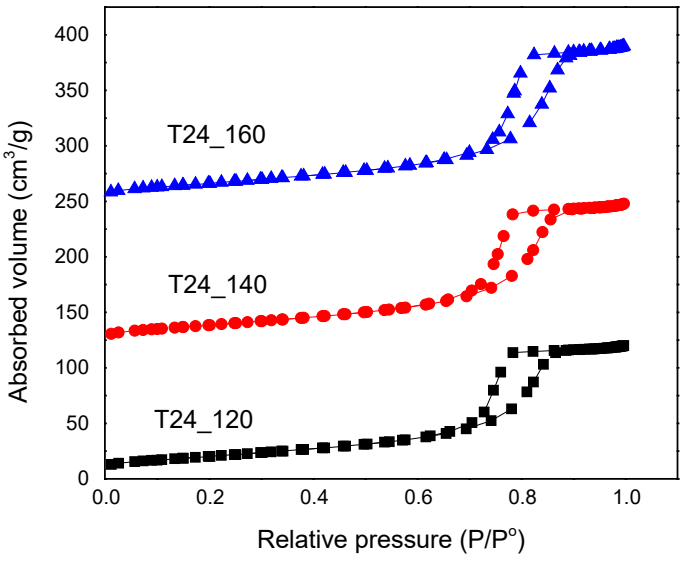

FIGURE 2. N_2 adsorption- desorption isotherm for T24_120, T24_140 and T24_160

TABLE 2. BET surface area, total pore volume and average pore size of T24_120, T24_140 and T24_160

Catalyst	BET surface area (m^2/g)	Pore volume (cm^3/g)	Average pore size (nm)
T24_120	74	0.18	7.35
T24_140	79	0.20	7.57
T24_160	77	0.23	8.43

CHARACTERIZATION OF FEEDSTOCK

The physicochemical properties of the feedstock which is acid value and water content has been determined. It is important to figure out the physicochemical properties of the feedstock as it can define the type of catalyst of catalyst and suitable reaction condition to get maximum yield (Olutoye & Hameed 2011). According to Table 3, the acid value of the feedstock is quite high from the standard value i.e. 1 mg KOH/g which require to do 2-step photocatalytic reaction which is photo-esterification followed by photo-transesterification. After the WCO undergo photo-esterification, the acid value reduced to 2.50 mg KOH/g.

TABLE 3. Physicochemical properties of WCO

Property	Unit	Value	Test method
Acid value	mg KOH/g	3.92	EN 14104
Water content	%	0.083	ASTM D6304

BIODIESEL PRODUCTION USING TIO_2 PHOTOCATALYSTS UNDER VISIBLE LIGHT IRRADIATION

The photocatalytic performance of the synthesized catalyst was tested during photo- transesterification reaction using esterified oil with FAME yield 0.65%. According to Figure 3, T24_160 shows best photocatalytic transesterification reaction provides higher biodiesel yield compared to other catalyst which is 3.41% in 1 h and 10 min with acid number 2.07 mg KOH/g. The higher biodiesel yield achieved using T24_160 could be due to higher amount of anatase phase which is 71.2% reported by the XRD result. Anatase phase of TiO_2 is known for having good photocatalytic activity (Fischer et al. 2017; Liao & Que 2010; Zhang et al. 2014). The photocatalytic activity increased with increasing anatase to rutile ratio but the ratio must be maintained below 80% anatase phase since sufficient rutile phase is required to maintain the electron-hole pair separation (Su et al. 2011). Besides, bigger pore size might be one of the reason as it could possess higher catalytic efficiency compared to the other synthesized catalyst (Ismail et al. 2016). According to other researchers, the large pore size is much more preferable as it can minimize the diffusion limitations for long alkyl chain hydrocarbons in FFA/TG in esterification and transesterification reactions (Gardy et al. 2016; Lam et al. 2009; Shu et al. 2010). On the other hand, it was reported that bigger pore size could facilitate the diffusion of the reactant (i.e. triglycerides) into the catalyst pore with active site in order to convert the compound to FAME (Hongmanorom et al. 2017). Intarasiri et al. (2017) also reported that larger pore size of cobalt supported mesoporous silica provides large active surface site that might promote the chain probability which led to production gasoline-diesel with selectivity 68.23%.

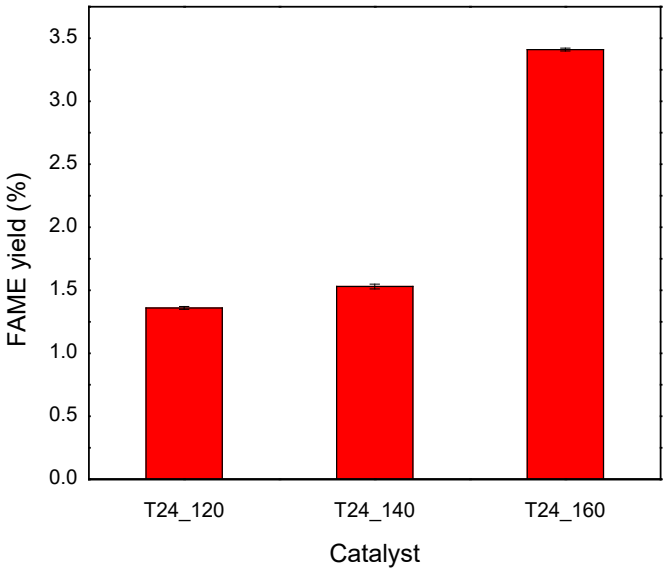

FIGURE 3. FAME yield in the biodiesel produced under visible light irradiation using H_2SO4 for photo- esterification meanwhile T24_120, T24_140 and T24_160 for photo- transesterification

Next, Figure 4 shows the fatty acid methyl ester (FAMEs) composition using different catalysts. Five types of FAME were detected in the biodiesel which are C12:0 (lauric acid methyl ester), C16:1 (palmitioleic acid methyl ester), C18:1 (oleic acid methyl ester), C18:2 (linoleic acid methyl ester) and C18:3 (linolenic acid methyl ester). Table 4 is the composition of FAMEs from previous study that have been done (Gardy et al. 2016). Comparing with our current study, it can been seen that the composition of FAMEs in synthesized biodiesel is much lower compared to other study. This might be due to the synthesis condition was not optimized yet, so optimization was based on catalyst loading, oil to methanol ratio and reaction time is needed in order to get high composition of FAMEs.

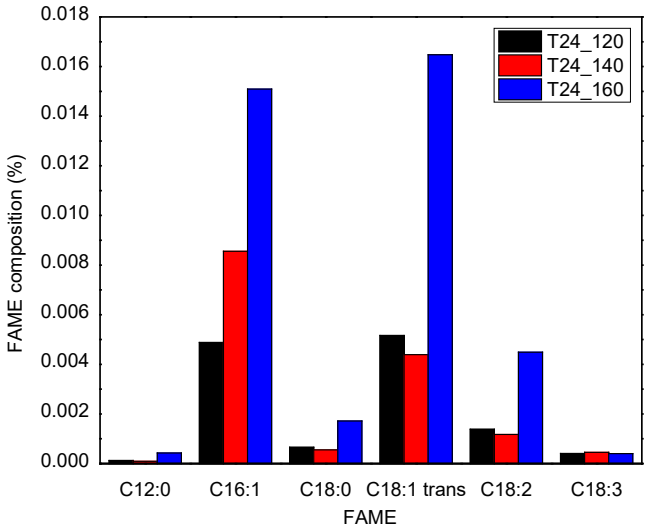

FIGURE 4. Composition of FAMEs in the biodiesel produced under visible light irradiation using T24_120, T24_140 and T24_160

TABLE 4. Composition of FAMEs from waste cooking oil

FAME	Form	Content (%)
Palmitic acid methyl ester	$C_{16:0}$	6.23
Stearic acid methyl ester	$C_{18:0}$	0.85
Oleic acid methyl ester	$C_{18:1}$	69.56
Linoleic acid methyl ester	$C_{18:2}$	20.41
Linolenic acid methyl ester	$C_{18:3}$	2.18
Arachidic acid methyl ester	$C_{20:0}$	0.17
Gadoleic acid methyl ester	$C_{20:1}$	0.31
Erucic acid methyl ester	$C_{21:1}$	0.16
Behenic acid methyl ester	$C_{22:0}$	0.12

Besides, Figure 5 shows the photo-generated electron-hole separation and charge transfer during photo-transesterification of esterified oil using T24_160 catalyst. Under irradiation of visible light, T24_160 catalyst is seen to absorbs more photon energy to excite the electron from valance band to conduction band more efficiently. The excitation of the electron to conduction will form a positively charged hole (h^+) which will oxidize methanol molecule, CH_3OH to form $CH_3O\cdot$ radical and hydrogen ions H^+. Next, the electron at the conduction band will be used to reduce triglyceride molecule, CH_2COOCR to form $CH_2COOCR\cdot$ radical similar as O_2 react with photogenerated e^- to form superoxide species. Then, the generated $CH_2COOCR\cdot$, $CH_3O\cdot$ and H^+ will react to form intermediates and final products (fatty acid methyl ester and diglyceride) as shown in the proposed mechanism scheme in Figure 6. The cycle will be continued until all the fatty acids convert to FAME and glycerol (by product).

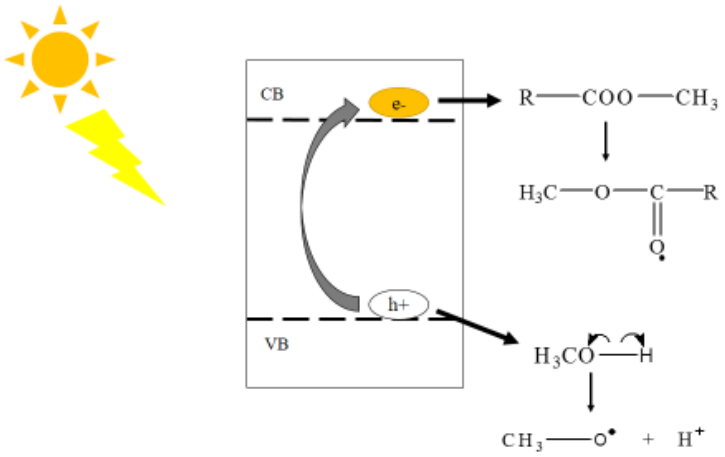

FIGURE 5. Charge transfer mechanism during photo-transesterification using T24_160

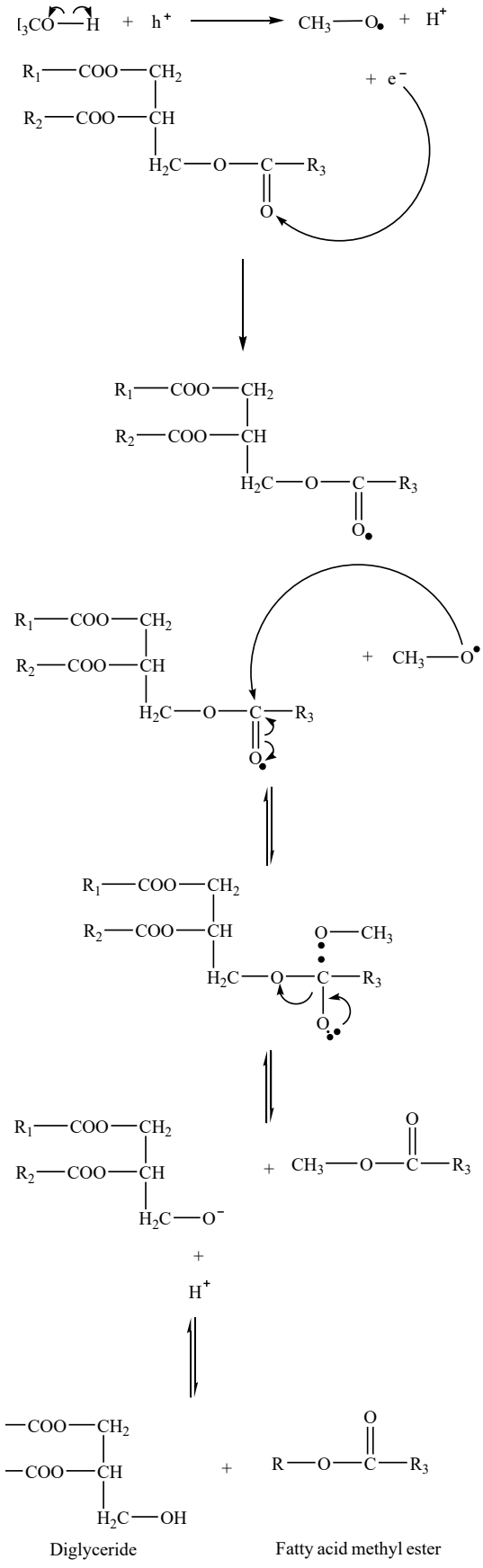

FIGURE 6. Proposed mechanism of photo-transesterification using synthesized T24_160 catalyst

Conclusion

Biodiesel was successfully produce from two-step photocatalytic reaction using waste cooking oil as the feedstock in the presence of H_2SO_4 used in photo-esterification followed by photo-transesterification using TiO_2. Highest biodiesel yield was achieved using T24_160 catalyst with yield 3.41%.

Acknowledgements

The authors are grateful for the funding provided by Yayasan Universiti Teknologi PETRONAS (YUTP, 015LC0-145).

References

Balat, M. & Balat, H. 2010. Progress in biodiesel processing. *Applied Energy* 87: 1815-1835.

Casallasa, I.D., Carvajal, E., Mahecha, E., Castrillón, C., Gómez, H., López, C. & Romero, D.M. 2018. Pre-treatment of waste cooking oils for biodiesel production. *Chemical Engineering Transaction* 65: 385-390.

Collazo, G.C., Jahn, S.L., Carreño, N.L.V. & Foletto, E.L. 2011. Temperature and reaction time effects on the structural properties of titanium dioxide nanopowders obtained via the hydrothermal method. *Brazilian Journal of Chemical Engineering* 28(2): 265-272.

Corro, G., Sanchez, N., Pal, U., Cebada, S. & Fierro, J.L.G. 2017. Solar-irradiation driven biodiesel production using Cr/SiO_2 photocatalyst exploiting cooperative interaction between Cr^{6+} and Cr^{3+} moieties. *Applied Catalysis B: Environmental* 203: 43-52.

Demirbas, A. 2005. Biodiesel production from vegetable oils via catalytic and non-catalytic supercritical methanol transesterification methods. *Progress in Energy and Combustion Science* 31(5-6): 466-487.

Demirbas, A. 2009. Progress and recent trends in biodiesel fuels. *Energy Conversion and Management* 50: 14-34.

Firoz, S. 2017. A review: Advantages and disadvantages of biodiesel. *International Research Journal of Engineering and Technology* 4(11): 530-535.

Fischer, K., Gawel, A., Rosen, D., Krause, M., Latif, A.A., Griebel, J., Prager, A. & Schulze, A. 2017. Low-temperature synthesis of anatase/rutile/brookite TiO_2 nanoparticles on a polymer membrane for photocatalysis. *Catalyst* 7: 209.

Fujishima, A. & Honda, K. 1972. Electrochemical photolysis of water at a semiconductor electrode. *Nature* 238: 37-38.

Gardy, J., Hassanpout, A., Lai, X. & Ahmed, M.H. 2016. Synthesis of $Ti(SO_4)O$ solid acid nano-catalyst and its application for biodiesel production from used cooking oil. *Applied Catalysis A: General* 557: 81-95.

Gashaw, A., Getachew, T. & Teshita, A. 2015. A review on biodiesel production as alternative fuel. *Journal of Forest Products & Industries* 4(2): 80-85.

Habibullah, M., Masjuki, H.H., Kalam, M.A., Rahman, S.M.A., Mofijur, M., Mobarak, H.M. & Ashraful, A.M. 2015. Potential of biodiesel as a renewable energy source in Bangladesh. *Renewable and Sustainable Energy Reviews* 50: 819-834.

Hongmanorom, P., Luengnaruemitchi, A., Chollacoop, N. & Yoshimura, Y. 2017. Effect of Pd/MCM-41 pore size on catalytic activity and cis-trans selectivity for partial hydrogenation of canola biodiesel. *Energy and Fuels* 31(8): 8202-8209.

Hussain, S., Jacob, J., Riaz, N., Mahmod, K., Ali, A., Amin, N., Nabi, G., Isa, M. & Mahmood, M.H.R. 2019. Effect of growth temperature on catalyst free hydrothermal synthesis of crystalline SnO_2 microsheets. *Ceramics International* 45(3): 4053-4058.

Hu, Y., Tsai, H.L. & Huang, C.L. 2003. Effect of brookite phase on the anatase-rutile transition in titania nanoparticles. *Journal of the European Ceramic Society* 23: 691-696.

Ibhadon, A.O. & Fitzpatrick, P. 2013. Heterogeneous photocatalysis: Recent advances and applications. *Catalysts* 3: 189-218.

Intarasiri, S., Ratana, T., Sornchamni, T., Phongaksorn, M. & Tungkamani, S. 2017. Effect of pore size diameter of cobalt supported catalyst on gasoline-diesel selectivity. *Energy Procedia* 138: 1035-1040.

Ismail, S., Ahmed, A.S., Anr, R. & Hamdan, S. 2016. Biodiesel production from Castor oil by using calcium oxide derived from mud clam shell. *Journal of Renewable Energy* 2016: Article ID. 5274917.

Kusdiana, D. & Saka, S. 2004. Effects of water on biodiesel fuel production by supercritical methanol treatment. *Bioresource Technology* 91(3): 289-295.

Lam, M.K., Lee, K.T. & Mohamed, A.R. 2009. Sulfated tin oxide as solid superacid catalyst for transesterification of waste cooking oil: An optimization study. *Applied Catalysis B: Environmental* 93(1-2): 34-139.

Lau, P.K., Kwong, T.L. & Yung, K.F. 2016. Effective heterogenous transition metal glycerolates catalyst for one-step biodiesel production from low grade non-refined *Jatropha* oil and crude aqueous bioethanol. *Scientific Reports* 6: 23822.

Lencka, M.M. & Riman, R.E. 1995. Thermodynamics of the hydrothermal synthesis of calcium titanate with reference to other alkaline-earth titanates. *Chemistry of Materials* 7: 18-25.

Liao, Y. & Que, W. 2010. Preparation and photocatalytic activity of TiO_2 nanotube powders derived by a rapid anodization process. *Journal of Alloys & Compounds* 505(1): 243- 248.

Lotero, E., Liu, Y., Lopez, D.E., Suwannakarn, K., Bruce, D.A. & Goodwin, J.G. 2005. Synthesis of biodiesel via acid catalysis. *Industrial and Engineering Chemistry Research* 44(14): 5353-5363.

Malligavathy, M., Iyyapushpam, S. & Nishanthi, S.T. 2018. Role of hydrothermal temperature on crystallinity,

photoluminescene, photocatalytic and gas sensing properties of TiO_2 nanoparticles. *Journal of Physics* 90: 44.

Mishra, V.K. & Goswami, R. 2018. A review of production, properties and advantages of biodiesel. *Biofuels* 9(2): 273-289.

Nakata, K. & Fujishima, A. 2012. TiO_2 photocatalysis: Design and applications. *Journal of Photochemistry & Photobiology C: Photochemistry Reviews* 13(3): 169-189.

Olutoye, M.A. & Hameed, B.H. 2011. Synthesis of fatty acid methyl ester from crude jatropha (*Jatropha curcas* Linnaeus) oil using aluminium oxide modified Mg-Zn heterogeneous catalyst. *Bioresource Technology* 102(11): 6392-6398.

Santhosh, C., Malathi, A., Daneshvar, A., Kollu, P. & Bhatnagar, P. 2018. Photocatalytic degradation of toxic aquatic pollutants by novel magnetic 3D-TiO_2@HPGA nanocomposite. *Scientific Report* 8: 1-15.

Sharma, A., Karn, R.K. & Pandiyan, S.K. 2014. Synthesis of TiO_2 nanoparticles by sol-gel method and their characterization. *Journal of Basic & Applied Engineering Research* 1(9): 1-5.

Scanlon, D.O., Dunnill, C.W., Buckeridge, J., Shevlin, S.A., Logsdail, A.J., Woodley, S.M., Catlow, C.R.A., Powell, M.J., Palgrave, R.G., Parkin, I.P., Watson, G.W., Keal, T.W., Sherwood, P., Walsh, A. & Sokol, A.A. 2013. Band alignment of rutile and anatase TiO_2. *Nature Materials* 12: 798-801.

Shu, Q., Gao, J., Nawaz, Z., Liao, Y., Wang, D. & Wang, J. 2010. Synthesis of biodiesel from waste vegetable oil with large amounts of free fatty acids using carbon-based solid acid catalyst. *Applied Energy* 87(8): 2589-2596.

Singh, I. & Birajdar, B. 2017. Synthesis, characterization and photocatalytic activity of mesoporous Na-doped TiO_2 nano-powder prepared via a solvent-controlled non-aqueous sol-gel route. *RSC Advances* 7: 54053.

Su, R., Bechstein, R., Sø, L., Vang, R.T., Sillassen, M., Esbjörnsson, B., Palmqvist, A. & Besenbacher, F. 2011. How the anatase- to- rutile ratio influences the photoreactivity of TiO_2. *Journal of Physical & Chemistry C* 115(49): 24287-24292.

Tan, K.T., Lee, K.T. & Mohamed, A.R. 2010. Effects of free fatty acids, water content and co solvent on biodiesel production by supercritical methanol reaction. *The Journal of Supercritical Fluids* 53(1-3): 88-91.

Tentu, R.D. & Basu, S. 2017. Photocatalytic water splitting for hydrogen production. *Current Opinion in Electrochemistry* 5: 56-62.

Tjandara, A.D. & Huang, J. 2018. Photocatalytic carbon dioxide reduction by photocatalyst innovation. *Chinese Chemical Letter* 29(6): 734-746.

Zhang, J., Zhou, P., Liu, J. & Yu, J. 2014. New understanding of the difference of photocatalytic activity among anatase, rutile and brookite TiO_2. *Physical Chemistry Chemical Physics* 16: 20382-20386.

Nurashina Abdul Rahman, Anita Ramli* & Chong Fai Kait
Department of Fundamental and Applied Sciences
Universiti Teknologi PETRONAS
32610 Seri Iskandar, Perak Darul Ridzuan
Malaysia

Anita Ramli*
HICoE
Centre for Biofuel and Biochemical Research
Institute of Self-Sustainable Building
Universiti Teknologi PETRONAS
32610 Seri Iskandar, Perak Darul Ridzuan
Malaysia

*Corresponding author; email: anita_ramli@utp.edu.my

Received: 7 July 2020
Accepted: 20 October 2020